N-Linked Glycosylation of the Human ABC Transporter ABCG2 on Asparagine 596 Is Not Essential for Expression, Transport Activity, or Trafficking to the Plasma Membrane†

Ndeye K. Diop and Christine A. Hrycyna*

Department of Chemistry and Purdue Cancer Center, Purdue University, 560 Oval Drive, West Lafayette, Indiana 47907-2084

Received September 17, 2004; Revised Manuscript Received January 3, 2005

ABSTRACT: The human ATP-binding cassette half-transporter ABCG2 is a 72 kDa plasma membrane protein that can confer multidrug resistance to cells in culture when overexpressed. Both transiently and stably expressed ABCG2 are glycosylated, and treatment with peptide *N*-glycosidase F reduces the apparent molecular mass on SDS−PAGE gels to approximately 60 kDa. Sequence analysis revealed three potential N-linked glycosylation sites in human ABCG2 at amino acids 418, 557, and 596. Site-directed mutagenesis experiments, in which each Asn was changed to Gln independently, revealed that only asparagine 596 is N-linked glycosylated. These data provide the first direct identification of the modified residue in ABCG2 and evidence for the localization of loop 5 to the extracellular space, previously only predicted from hydropathy analysis. Immunoblot and pulse-chase analyses revealed that the glycosylation-deficient ABCG2 (N596Q) variant and the glycosylated parent transporter are expressed equivalently at steady state and have similar half-lives. Cell surface analysis of ABCG2 expression showed comparable amounts of the N596Q variant present at the plasma membrane compared to the glycosylated ABCG2 protein. The ABCG2 (N596Q) variant is also functional, demonstrating rhodamine 123 transport in intact cells comparable to that in cells expressing glycosylated ABCG2. Furthermore, in crude membrane preparations, neither the basal nor the prazosin-stimulated (∼2-fold) ATPase activities of ABCG2 (N596Q) were affected compared to glycosylated ABCG2. Although subtle defects in transporter trafficking and function may exist, these data taken together suggest that N-glycosylation at arginine 596 is not essential for the expression, trafficking to the plasma membrane, or the overall function of ABCG2.

A major obstacle encountered in cancer treatment is the existence or development of resistance to multiple anti-cancer drugs. Some characteristics of the multidrug resistance phenotype include a decrease in intracellular drug levels and overexpression of members of the ATP-binding cassette (ABC)[1] superfamily of membrane transporters (*1*, *2*). This superfamily is comprised of hundreds of proteins in both prokaryotic and eukaryotic organisms, most of which are involved in ATP-driven transmembrane transport of diverse compounds either into or out of cells (*3*). ABC transporters known to be involved in mammalian multidrug resistance are P-glycoprotein (P-gp) encoded by the *MDR*1 gene in humans (*4*), the multidrug resistance-associated proteins (MRPs) encoded by the MRP genes (*5*), and the more recently identified ABCG2, also known as MXR1 (*6*), BCRP (*7*), and ABCP (*8*).

ABCG2 was first cloned from drug-resistant breast cancer and colon cancer cell lines selected in mitoxantrone or doxorubicin (*6*−*8*). ABCG2, a 655 amino acid glycoprotein with a predicted molecular mass of 72 kDa, is a member of the G-subfamily of human ABC transporters that contain only one transmembrane domain comprised of six transmembrane segments and one nucleotide binding domain (*8*, *9*). The ATP-binding cassette (ABC) is found at the N-terminus, and the C-terminal transmembrane domain is predicted to span the membrane six times (Figure 1). Since a complete and functional ABC transporter contains at least twelve transmembrane segments and two ATP-binding domains, ABCG2 is called a "half-transporter" and is thought to form a dimer or higher order oligomer in order to function (*10*−*12*).

Three forms of ABCG2 containing Arg, Gly, or Thr at amino acid position 482 were isolated from different drug-selected human tumor cells. Arginine 482 (R482) has been reported in the literature as the wild-type form of ABCG2, while glycine 482 (R482G) and threonine 482 (R482T) arose as a result of drug selection (*6*−*8*). Wild-type ABCG2 is normally expressed in multiple tissues including the placenta, small intestine, liver, brain microvessel endothelium, colon, bile canaliculi, breast, and stem cells (*13*−*18*). From these localization data, it has been hypothesized that ABCG2 might play an important role in eliminating toxic exogenous compounds, protecting the fetus during development, as well as effluxing maturation factors from undifferentiated stem cells (*8*, *15*, *18*−*21*). Furthermore, it has recently been demonstrated that cells expressing ABCG2 are able to transport steroid hormones, including estrogens (*22*−*24*).

† This work was supported in part by American Cancer Society Institutional Research Grant IRG-58-006-41 to the Purdue University Cancer Center.

* Corresponding author. Phone: 765-494-7322. Fax: 765-494-0239. E-mail: hrycyna@purdue.edu.

[1] Abbreviations: PNGase F, peptide *N*-glycosidase F; ABC, ATP-binding cassette; P-gp, P-glycoprotein; FITC, fluorescein isothiocyanate; SDS−PAGE, sodium dodecyl sulfate−polyacrylamide gel electrophoresis; ER, endoplasmic reticulum; Endo H, endoglycosidase H; FACS, fluorescence-activated cell sorting.

10.1021/bi0479858 CCC: $30.25
Published on Web 03/15/2005

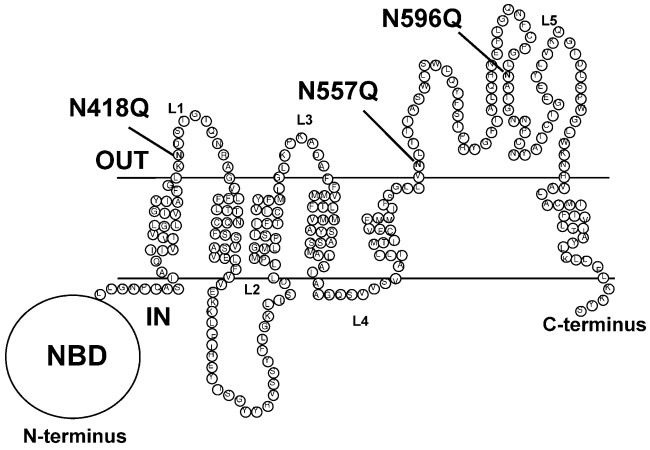

FIGURE 1: Two-dimensional hypothetical topology model of human ABCG2. Hydropathy analysis of the amino acid sequence of ABCG2 suggests that the protein consists of six transmembrane domains (amino acids 396−416, 429−449, 478−498, 507−527, 536−556, and 631−651), one nucleotide binding domain (NBD) located at the N-terminus (amino acids 1−388), and three potential N-linked glycosylation sites located in the first and third extracellular loops (L1 and L5) at positions N418, N557, and N596 (modified from ref *9*).

Analysis of the primary sequence of ABCG2 reveals three potential extracellular N-linked glycosylation sites with the consensus sequence Asn-X-Thr/Ser, where X can be any amino acid except proline (*25*). The fourth possible consensus sequence for N-linked glycosylation in ABCG2 is believed not to be exposed to the lumen of the endoplasmic reticulum and thus not potentially glycosylated. All three potentially modified sites are located in the first and third putative extracellular loops (L1 and L5) at amino acid residues Asn 418, Asn 557, and Asn 596 (Figure 1). In this study, we identified Asn 596 as the single N-linked glycosylated amino acid in ABCG2 using chemical treatments with tunicamycin or PNGase F and site-directed mutagenesis, constructing and evaluating three N → Q variants (N418Q, N557Q, and N596Q). The glycosylation-deficient ABCG2 (N596Q) is expressed at similar cell surface and steady-state levels as the glycosylated protein and has a similar half-life. Furthermore, ABCG2 (N596Q) is functional for both basal and drug-stimulated ATPase activity as well as for drug transport in intact cells, comparable to glycosylated ABCG2. These data suggest that N-linked glycosylation of ABCG2 is not essential for ABCG2 expression, trafficking to the plasma membrane, or the overall function of ABCG2, although subtle defects in any of these processes may exist.

EXPERIMENTAL PROCEDURES

Materials. Dulbecco's modified Eagle's medium (DMEM), fetal bovine serum (FBS), and calf serum (CS) were purchased from BioWhittaker (Cambrex, Walkersville, MD). L-Glutamine, trypsin−EDTA, and penicillin/streptomycin were obtained from MediaTech Cellgro (Herndon, VA). Lipofectin RPMI1640 and Opti-MEM I were purchased from Invitrogen Life Technologies/Gibco (Carlsbad, CA). Prazosin, rhodamine 123, doxorubicin (adriamycin), verapamil, sodium orthovanadate, ATP, oubain, and EGTA were purchased from Sigma-Aldrich (St. Louis, MO). PCR primers were ordered from Integrated DNA Technologies, Inc. (Coralville, IA). Restriction enzymes and peptide *N*-glycosidase F (PNGase F) were obtained from New England BioLabs (Beverly, MA). Tunicamycin, bestatin, pepstatin, and chymostatin were bought from MP Biomedicals, Inc. (Aurora, OH). Dithiothreitol (DTT), AEBSF, and aprotinin were purchased from Fisher Scientific (Pittsburgh, PA). Sodium dodecyl sulfate (SDS) was obtained from Bio-Rad Laboratories (Hercules, CA), and micrococcal nuclease was purchased from Worthington (Lakewood, NJ). The pTM1 vector was a gift from Dr. B. Moss (NIAID, NIH, Bethesda, MD), and the recombinant vaccinia virus encoding bacteriophage T7 RNA polymerase (vTF7-3) was a gift from Dr. Steven Broyles (Purdue University). MCF-7/AdVp3000 cells were generously provided by Dr. Susan Bates (NCI, NIH). Monoclonal antibodies BXP-21 and 5D3 were obtained from Kamiya Biomedical Co. (Seattle, WA) and Chemicon International (Temecula, CA), respectively.

Construction of ABCG2 Glycosylation Mutants. To create N-glycosylation mutants, the asparagine (N) residue within the consensus sequence NX(S/T) was replaced with a glutamine (Q). Single point mutations were introduced by sequence overlap extension (SOE) PCR using pTM1-ABCG2 (R482G) DNA as the expression vector template. The following genetic variants were obtained: Asn 418 (N418Q), Asn 557 (N557Q), and Asn 596 (N596Q). The final product was fully sequenced in both directions to ensure fidelity and proper introduction of the mutations.

Cell Lines. HeLa cells (cervical epitheloid carcinoma) were propagated as a monolayer at 37 °C, 5% CO_2, in high-glucose DMEM supplemented with 2 mM L-glutamine, 50 units/mL penicillin, 50 μg/mL streptomycin, and 10% FBS. The drug-resistant breast adenocarcinoma cell line, MCF-7/AdVp3000 (*6*), was maintained in RPMI1640 supplemented with 2 mM L-glutamine, 50 units/mL penicillin, 50 μg/mL streptomycin, and 10% FBS plus 3 μg/mL adriamycin and 5 μg/mL verapamil.

Transient Vaccinia Virus Expression System. Cells were transiently transfected and infected as previously described (*26*). A 70−80% confluent monolayer of HeLa cells was infected with the vTF 7-3 vaccinia virus (10 pfu/cell) and cotransfected with an appropriate amount of a pTM1 expression plasmid containing ABCG2 or the following ABCG2 variants: N418Q, N557Q, and N596Q. The empty vector, pTM1, was used as a negative control. Cells were fed 4 h post-infection/transfection with complete DMEM culture media and incubated for 15−48 h at 32 °C in a humidified atmosphere of 5% CO_2 in air.

Crude Membrane Isolation. Crude membranes were prepared 48 h post-infection/transfection by hypotonic lysis as described previously (*26*). Briefly, HeLa cells were harvested by scraping and washed with phosphate-buffered saline (PBS), pH 7.4, supplemented with 1% (v/v) aprotinin. Cells were harvested by centrifugation at 450*g* and 4 °C, resuspended in lysis buffer [10 mM Tris, pH 7.5, 10 mM NaCl, 1 mM $MgCl_2$, 2 mM AEBSF, 1 mM DTT, 1% (v/v) aprotinin], and homogenized using a Dounce homogenizer (Pestle A). Following centrifugation at 450*g* for 10 min, the supernatant was collected and treated on ice for 20 min with 1 mM $CaCl_2$ and 50 units/mL micrococcal nuclease. Crude membranes were isolated by centrifugation at 300000*g* for 40 min at 4 °C. The pellet was resuspended in TSNa buffer [10 mM Tris, pH 7.5, 50 mM NaCl, 250 mM sucrose, 2 mM AEBSF, 1 mM DTT, 1% (v/v) aprotinin, 10% (v/v)

glycerol], and the protein concentration was quantified. Aliquots of the crude membranes were stored at −80 °C.

Flow Cytometric Analysis. Cell surface expression and substrate accumulation studies were performed as previously described (*26*), with slight modifications. Fifteen to twenty-one hours post-infection/transfection, cells were trypsinized, harvested, and resuspended in media containing 5% (v/v) calf serum. Cell surface expression of ABCG2 and ABCG2 variants was detected in HeLa cells (500000) by labeling with the monoclonal antibody 5D3 (2 μg) (*27*), washing, and subsequent labeling with an anti-mouse FITC-conjugated IgG secondary antibody (2 μg). Cells were harvested by centrifugation and resuspended in 300 μL of ice-cold PBS prior to flow cytometric analysis. For rhodamine 123 transport assays, 500000 HeLa cells were incubated with 0.5 μg/mL rhodamine 123 for 40 min at 37 °C. Cells were then harvested at 300*g*, resuspended in drug-free culture media, and incubated for an additional 10−66 min at 37 °C. Cells were harvested and resuspended in 300 μL of ice-cold PBS and subjected to flow cytometric analysis. A FACS Calibur flow cytometer (Becton-Dickinson, San Jose, CA) equipped with a 488 nm argon laser and a 530 nm band-pass filter (FL1) was used for detection of FITC labeling and rhodamine 123 accumulation. CellQuest software (Becton-Dickinson, San Jose, CA) was used for acquiring and analyzing the data.

Chemical Analysis of N-Linked Glycosylation. For inhibition of *de novo* N-linked glycosylation, HeLa cells were infected and cotransfected with the appropriate expression plasmid in the presence of 5 μg/mL tunicamycin. After 4 h, cells were further incubated for 15−21 h in complete medium supplemented with 5 μg/mL tunicamycin. Enzymatic deglycosylation in crude membranes (10−40 μg) was performed using PNGase F, following the manufacturer's protocol with the addition of protease inhibitors [10 μg/mL bestatin, 10 μg/mL pepstatin, 10 μg/mL chymostatin, 1% (v/v) aprotinin, and 2 mM AEBSF]. The reaction was stopped by the addition of 5× Laemmli sample buffer, and the samples were subsequently subjected to SDS−PAGE and immunoblot analysis as described below. To distinguish between core and complex protein N-glycosylation, crude membrane preparations were treated with endoglycosidase H (Endo H; Roche Diagnostics Corp., Indianapolis, IN). Total membrane protein (20−40 μg) was incubated in 20 mM sodium acetate, pH 5.0, 1× denaturing buffer (0.05% SDS and 0.1% β-mercaptoethanol), protease inhibitors [10 μg/mL bestatin, 10 μg/mL pepstatin, 10 μg/mL chymostatin, 1% (v/v) aprotinin, and 2 mM AEBSF], 1× NP-40, and 1× reaction buffer (50 mM $NaCH_3COO$ and 25 mM EDTA) in the presence or absence of Endo H (10 milliunits) for 2 h at 37 °C. Reactions were stopped by the addition of an appropriate amount of 5× Laemmli sample buffer and incubated at room temperature for 30 min. The samples were subsequently subjected to 10% SDS−PAGE and immunoblot analysis.

SDS−PAGE and Immunoblot Analysis. SDS−PAGE samples were separated on 10% Tris−glycine gels and transferred to a 0.45 μm PROTRAN nitrocellulose membrane (Schleicher & Schuell BioScience Inc., Keene, NH). The membrane was blocked with 20% (w/v) nonfat dry milk dissolved in PBS supplemented with 0.05% (v/v) Tween 20 (PBST) and then incubated with the anti-ABCG2 monoclonal antibody BXP-21 (1:2000 dilution) (*15*) in a 5% (w/v) nonfat dry milk solution in PBST. After being washed with PBST, the blot was incubated with anti-mouse IgG−HRP-conjugated secondary antibody (1:4000 dilution) in a 5% (w/v) nonfat dry milk solution in PBST, washed, and developed with SuperSignal West Pico enhanced chemiluminescent (ECL) reagents (Pierce Biotechnology, Rockford, IL).

^{35}S-Trans Labeling of Vaccinia Virus Infected/Transfected HeLa Cells. Twenty hours post-infection/transfection, HeLa cells plated in 35 mm dishes expressing ABCG2 or the glycosylation-deficient mutant ABCG2 (N596Q) were washed twice with 1× PBS and once with DMEM supplemented with FBS and Gln but without methionine and cysteine (DMEM [(−) Cys, (−) Met]) and then preincubated in 1 mL of DMEM [(−) Cys, (−) Met] for 5 min. ^{35}S-trans label (final concentration 40 μCi/mL) (MP Biomedicals, Inc., Irvine, CA) was then added, and the cells were incubated at 32 °C for 1 h. Labeled cells were washed three times with warm (32 °C) 1× PBS. Control cells at the zero ("0") time point were rapidly washed with ice-cold 1× PBS before being lysed in RIPA buffer (0.1% SDS, 1% Triton X-100, 1% sodium deoxycholate, and 2 mM EDTA in PBS, pH 7.4) containing protease inhibitors [1% (v/v) aprotinin and 2 mM AEBSF] for 30 min. Cells in the other wells were further incubated (chased) with 2 mL of complete DMEM medium for 3, 6, 9, 18, 19, and 20 h at 32 °C. Cells were harvested at the indicated time points, the ABCG2 proteins were immunoprecipitated with the monoclonal antibody BXP-21, and the samples were analyzed by SDS−PAGE and autoradiography.

Immunoprecipitation. Cell lysates were prepared in RIPA buffer (0.1% SDS, 1% Triton X-100, 1% sodium deoxycholate, and 2 mM EDTA in PBS, pH 7.4) containing protease inhibitors (1% aprotinin and 2 mM AEBSF). One milliliter of total cell lysate was incubated with 2.5 μg of BXP-21 monoclonal antibody overnight at 4 °C with rotation. Protein A−Sepharose beads (Amersham Biosciences, Piscataway, NJ) were pre-washed twice in RIPA buffer containing protease inhibitors, added to the reactions, and allowed to incubate at 4 °C for at least 4 h with rotation. The bead complex was harvested by centrifugation for 10 s in a microcentrifuge at top speed and washed three times in RIPA buffer containing protease inhibitors. After the final wash, 1× SDS sample buffer was added to the beads and allowed to incubate at room temperature for 30 min. The beads were removed by centrifugation, and the supernatant was subjected to SDS−PAGE on a 10% polyacrylamide gel. The gel was fixed in 10% (v/v) glacial acetic acid and 30% (v/v) methanol for 45 min at room temperature and then impregnated with ENLIGHTNING (Perkin-Elmer Life and Analytical Sciences, Boston, MA) for 20−30 min at room temperature. The gel was dried under vacuum at a temperature of 75 °C for 90 min. The dried gel was exposed to X-ray film at −80 °C for 2−3 days to achieve the desired exposure. Alternatively, the radioactivity associated with ABCG2 was quantified using a phosphorimager.

Immunofluorescence Confocal Microscopy. HeLa cells expressing either ABCG2 or ABCG2 (N596Q) were harvested 17 h post-infection/transfection and resuspended in 1 mL of 1× PBS. Cells were fixed, but not permeabilized, for 10 min in methanol at room temperature. After fixation, cells were harvested by centrifugation at 500*g* and washed

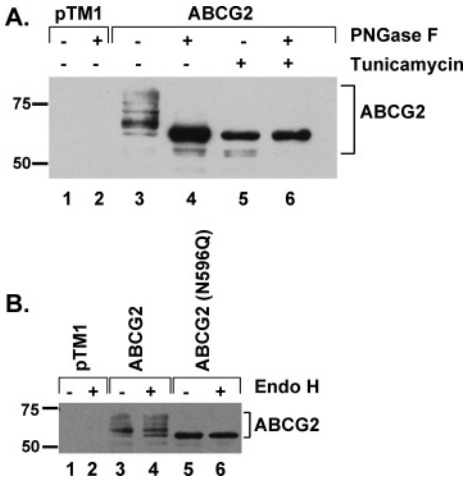

FIGURE 2: Immunoblot analysis of expression of ABCG2 proteins in transiently transfected HeLa cells. (A) HeLa cells were co-transfected/infected with the pTM1 negative control plasmid or pTM1-ABCG2 and incubated in the presence (+) or absence (−) of tunicamycin (5 μg/mL) for 48 h. Crude membranes derived from these cells were subsequently treated with (+) or without (−) PNGase F. (B) HeLa cells were co-transfected/infected with the pTM1 negative control plasmid, pTM1-ABCG2 or pTM1-ABCG2 (N596Q), in the absence of tunicamycin for 48 h. Crude membranes derived from these cells were subsequently treated with (+) or without (−) Endo H. All samples (10 μg of total protein) were subjected to SDS−PAGE on 10% Laemmli-type gels (*55*), followed by immunoblotting with the monoclonal antibody BXP-21 (1:2000). ABCG2 proteins were visualized as described in Experimental Procedures. The positions of ABCG2 are denoted by a bracket.

once with 1× PBS. The cells were incubated with the ABCG2 cell surface specific monoclonal antibody 5D3 at a 1:100 dilution in 1× PBS plus 0.5% BSA for 2 h at 37 °C. After being washed twice with 1× PBS, the cells were incubated in a 1:100 dilution of a FITC-labeled anti-mouse antibody in 1× PBS plus 0.5% BSA for 45 min at 37 °C. Cells were rinsed three times with 1× PBS and analyzed by confocal microscopy. A Bio-Rad MRC 1024 confocal laser scanning microscope equipped with an Ar−Kr laser exciting at 488 nm was used for excitation of the fluorescein label, and the emitted light passed through a 522−535 nm band-pass filter.

ATPase Activity Measurement. Crude membranes were analyzed for basal and prazosin-stimulated ATPase hydrolysis by colorimetric detection of inorganic phosphate liberation from Mg^{2+}-ATP as described previously (*26*).

RESULTS

ABCG2 Is Modified by N-Linked Glycosylation. The ABCG2 protein variant R482G was chosen for this study because it has broader substrate specificity than the wild-type ABCG2 (R482) and can transport the dye rhodamine 123, our model substrate (*28*). All N-glycosylation variants constructed and described here have ABCG2 (R482G) as the protein backbone, and in this study, the ABCG2 designation will refer to the ABCG2 (R482G) protein unless otherwise specified. We chose to use HeLa cells because of their low endogenous expression of ABCG2 (Figure 2, lanes 1 and 2). Cells were co-infected with vTF7-3 recombinant vaccinia virus expressing bacteriophage T7 RNA polymerase and simultaneously transfected with either the pTM1 vector alone (negative control) or the pTM1 vector containing the full-length ABCG2 cDNA for 20−24 h. Immunoblot analysis demonstrated that ABCG2 was expressed efficiently in HeLa cells (Figure 2A, lane 3), with none detected in the negative control pTM1-transfected cells (Figure 2A, lanes 1 and 2). Although the majority of the ABCG2 protein migrates at approximately 72 kDa, minor amounts of higher molecular mass species are also observed, whose exact pattern can vary between experiments depending upon the amount of protein loaded on the gel and the age of the membrane preparation. This heterogeneity can be attributed to differential glycosylation of the protein, due to the rapid rate of protein synthesis (*29*). Similar migration patterns are observed for wild-type ABCG2 and the R482T variant (data not shown).

Upon treatment of ABCG2-expressing HeLa cell crude membranes with PNGase F, an amidase that cleaves between the innermost GlcNAc and asparagine residues of high-mannose, hybrid, and complex oligosaccharides from N-linked glycoproteins, a single band at a lower apparent molecular mass at approximately 60 kDa was observed (Figure 2A, lane 4). These data suggest that ABCG2 expressed in these cells is modified by N-linked glycosylation, as has been observed previously in stable cell lines expressing ABCG2 (*11*). Small amounts of protein species are observed below the major band, which may be attributed to minor degradation products. To determine whether the reduction in apparent molecular mass was due solely to the enzymatic deglycosylation of ABCG2 by PNGase F, tunicamycin, a known inhibitor of *de novo* N-linked glycosylation, was used in the growth medium of the cells during expression. Crude membranes derived from cells expressing ABCG2 in the presence of tunicamycin (Figure 2A, lane 5) showed a homogeneous protein population at a molecular mass that co-migrated with the PNGase F treated sample (Figure 2A, lane 4). No further reduction in the apparent molecular mass of the ABCG2 protein expressed in the presence of tunicamycin was observed upon further treatment with PNGase F (Figure 2A, lane 6). Taken together, these data demonstrate that ABCG2 is N-linked glycosylated and that PNGase F treatment or the presence of tunicamycin during protein synthesis results in a protein that is devoid of N-linked glycosylation.

The heterogeneity of glycosylation observed for ABCG2 expressed in the HeLa cells using the vaccinia virus expression system was evaluated further using endoglycosidase H (Endo H), an enzyme that removes sugars from proteins that are modified by high-mannose and some hybrid glycans. Crude membranes derived from cells expressing glycosylated ABCG2 treated with Endo H ran similarly to the untreated sample, demonstrating that the majority of the protein species are Endo H insensitive (Figure 2B, lane 4). However, a modest increase in the 60 kDa band representing fully deglycosylated ABCG2 was observed. Together, these data suggest that the majority of the ABCG2 produced in these cells has been at least partially modified by further complex glycosylation. Confocal microscopy in permeablized cells shows a substantial amount of ABCG2 protein retained within the cells in a punctuate pattern (data not shown). Taken together with the Endo H insensitivity results above, these data suggest that most of the internal protein, present presumably because of the rapid rate of synthesis in the vaccinia virus expression system, is most likely associated with post-ER/*cis*-Golgi compartments.

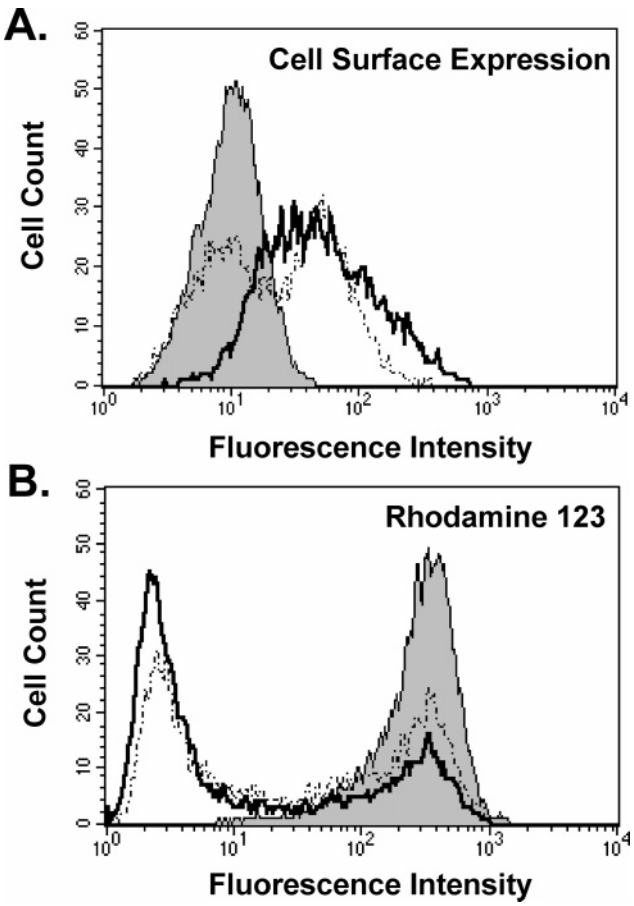

FIGURE 3: Cell surface localization and rhodamine 123 accumulation of ABCG2 in the presence and absence of tunicamycin. HeLa cells were cotransfected/infected with empty vector pTM1 (shaded) or pTM1-ABCG2 in the presence (- - -) or absence (—) of 5 μg/mL tunicamycin. (A) Cell surface localization of ABCG2: Cells were stained with the external epitope-specific monoclonal antibody, 5D3, followed by the anti-mouse IgG FITC-conjugated secondary antibody, and subjected to flow cytometric analysis as described in Experimental Procedures. (B) Rhodamine 123 accumulation: Cells were incubated at 37 °C for 40 min with 0.5 μg/mL rhodamine 123. After incubation, cells were harvested by centrifugation, resuspended, incubated in drug-free medium for an additional 40 min at 37 °C, and subjected to flow cytometric analysis as described in Experimental Procedures. Each histogram is based on a sample of 10000 cells, and each experiment was performed a minimum of three independent times.

Glycosylation-Deficient ABCG2 Is Functional and Is Expressed at the Cell Surface. Since ABCG2 is normally localized to the plasma membrane, we evaluated the cell surface expression of both the glycosylated and the glycosylation-deficient ABCG2 proteins by flow cytometry using the monoclonal antibody 5D3 that specifically recognizes an external epitope on human ABCG2 (*27*) and a FITC-conjugated secondary antibody. HeLa cells were co-infected/transfected with either the empty pTM1 control plasmid or pTM1 containing the ABCG2 cDNA and incubated for 18 h in the absence or presence of 5 μg/mL tunicamycin. In the absence and presence of tunicamycin, respectively, both fully glycosylated ABCG2 and the glycosylation-deficient protein were expressed at the cell surface, as demonstrated by an increase in fluorescence intensity compared to the negative pTM1 control (Figure 3A). The two peaks observed in the tunicamycin-treated cells, and to a lesser extent in the untreated cells, represent two different cell populations that express different amounts of ABCG2. In fact, the left peak in the tunicamycin-treated cells is superimposed upon the negative pTM1 control, suggesting little to no ABCG2 expression in these cells (Figure 3A). Given that all other variables were held constant, these data suggest that the tunicamycin may have prevented either efficient transfection or expression of the plasmid and not necessarily an inherent difference in protein stability or in the ability of the glycosylation-deficient protein to traffic to the cell surface.

The Glycosylation-Deficient ABCG2 Protein Expressed in the Presence of Tunicamycin Retains Transport Activity. The ability of the glycosylation-deficient ABCG2 to transport rhodamine 123 was assessed and compared to glycosylated ABCG2. HeLa cells were transiently infected with vTF7-3 and transfected with ABCG2 or pTM1 as a negative control. Parallel cultures of ABCG2 expressing cells were incubated in the presence and absence of 5 μg/mL tunicamycin for 18 h and assayed for rhodamine 123 accumulation as described in Experimental Procedures. The cells expressing the glycosylation-deficient ABCG2, expressed in the presence of tunicamycin, exclude rhodamine 123 similarly to cells expressing the glycosylated protein (Figure 3B). These data suggest that glycosylation is not essential for the substrate transport activity of ABCG2.

Human ABCG2 Is Glycosylated at Asn 596, Located in the Third Extracellular Loop of ABCG2. The sequence and predicted membrane topology of the ABCG2 multidrug transporter suggests three possible N-linked glycosylation sites at asparagines 418, 557, and 596 (Figure 1). Site-directed mutagenesis was performed on the human ABCG2 cDNA to generate three mutant variants of the half-transporter where the Asn residues were replaced by Gln residues: ABCG2 (N418Q), ABCG2 (N557Q), and ABCG2 (N596Q). HeLa cells were infected with the vTF7-3 vaccinia virus and transfected with the respective human ABCG2 vectors containing the variant cDNAs. The expression level of ABCG2 and the ABCG2 mutant variants in crude total membrane preparations from these cells was detected by immunoblot analysis using the monoclonal antibody BXP-21 (*15*). ABCG2 (N418Q) and ABCG2 (N557Q) migrated as a range of bands between the 50 and 75 kDa markers and are indistinguishable from the glycosylated ABCG2 control (Figure 4A, lanes 1, 3, and 5). However, ABCG2 (N596Q) migrated as a single species at ~60 kDa (Figure 4A, lane 7). In the stable drug-selected cell line MCF-7/AdVp3000 that overexpresses ABCG2 (R482T), the protein also migrates as a single species but at a higher molecular mass closer to the 75 kDa marker (Figure 4B, lane 1). Upon treatment of both the HeLa and MCF-7/AdVp3000 membrane preparations with PNGase F, the ABCG2 proteins migrated to approximately the same lower molecular mass position (~60 kDa) (Figure 4A,B, lanes 2). These data confirm our hypothesis that the range of ABCG2-specific bands seen in the transiently expressed HeLa cells represents different glycosylated forms of the protein (Figures 2 and 4). Upon treatment with PNGase F, both ABCG2 variants N418Q (Figure 4A, lane 4) and N557Q (Figure 4A, lane 6) also migrate to the same lower molecular mass position (~60 kDa) as the PNGase F treated ABCG2 glycosylated protein and the untreated N596Q protein (Figure 4A, lanes 2, 4, 6, and 7). In addition, no further reduction in the molecular mass of ABCG2 (N596Q) was observed upon

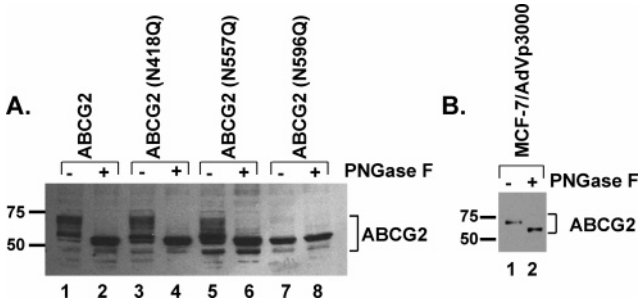

FIGURE 4: Immunoblot detection of ABCG2 and the N418Q, N557Q, and N596Q ABCG2 variants. (A) Crude membranes (20 μg of total protein) derived from HeLa cells co-transfected/infected with the pTM1 (negative control) or the ABCG2 variants independently were treated with (+) or without (−) PNGase F, and 10 μg of protein was subjected to SDS−PAGE on 10% Laemmli-type gels (*55*). (B) Crude membranes derived from MCF-7/AdVp3000 cells (10 μg) overexpressing ABCG2 (R482T) were treated with (+) or without (−) PNGase F. Two micrograms of total protein was subjected to SDS−PAGE on 10% Laemmli-type gels followed by immunoblot analysis with the BXP-21 monoclonal antibody. ABCG2 proteins were visualized as described in Experimental Procedures. The position of ABCG2 is denoted by a bracket.

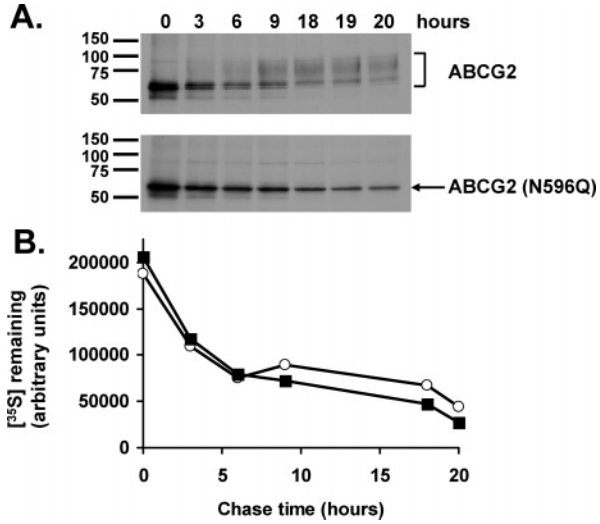

FIGURE 5: Synthesis and degradation of ABCG2 and glycosylation-deficient ABCG2 (N596Q) in transiently transfected HeLa cells. (A) ABCG2 and ABCG2 (N596Q) expressing HeLa cells were pulsed with a ^{35}S-trans label in DMEM lacking cysteine and methionine. After washing, cells were chased in complete DMEM for the indicated times (0, 3, 6, 9, 18, 19, 20 h), harvested, and lysed in RIPA buffer as described in Experimental Procedures. Control cells at the zero (0) time point were rapidly washed with ice-cold 1× PBS before lysing in RIPA buffer. ABCG2 proteins were immunoprecipitated with the monoclonal antibody BXP-21, and the samples were analyzed by SDS−PAGE and autoradiography. (B) Quantitation of ^{35}S-trans label incorporation into ABCG2 and ABCG2 (N596Q). The SDS−PAGE gels shown in panel A were subjected to phosphorimager analysis. For the glycosylated ABCG2 sample, the signals from all of the molecular mass ABCG2 species (shown by the bracket in panel A) were measured. For ABCG2 (N596Q), only the signal from the ~60 kDa band was measured, as this variant is expressed as a single species.

treatment with PNGase F (Figure 4A, lane 8), indicating that this variant is not modified by N-linked glycosylation. Furthermore, treatment with Endo H had no effect on the mobility of ABCG2 (N596Q), demonstrating that the protein does not possess even core glycosylation features (Figure 2B, lane 6). Taken together, these data demonstrate that human ABCG2 is normally N-linked glycosylated only at asparagine 596 (N596) and establish that this region of the protein is localized to the extracellular space, as predicted by topology models (Figure 1).

The Glycosylation-Deficient Mutant ABCG2 (N596Q) and Glycosylated ABCG2 Proteins Are Expressed Equivalently at Steady State and Have Similar Cellular Half-Lives. To determine if ABCG2 and ABCG2 (N596Q) proteins were expressed at similar steady-state levels and have similar half-lives, pulse-chase experiments were performed in vaccinia virus transfected/infected HeLa cells. The cells were starved in DMEM medium without cysteine or methionine, incubated in the presence of ^{35}S-trans label (pulse), and chased in complete DMEM medium for a maximum of 20 h, as described in Experimental Procedures. ABCG2 proteins were immunoprecipitated using the monoclonal antibody BXP-21 and subjected to SDS−PAGE and autoradiography. As shown in Figure 5A (top panel), glycosylated ABCG2 is initially synthesized as the 60 kDa precursor and matures over time to the more heterogeneous mixture of differentially glycosylated proteins. The nonglycosylated ABCG2 (N596Q) is only expressed as the 60 kDa species (Figure 5A, bottom panel). Using a phosphorimager to quantitate the amount of label present in the proteins over time, we determined that the initial incorporation of the ^{35}S-trans label was similar for both the glycosylated and nonglycosylated ABCG2 proteins (Figure 5B), indicating that they are being expressed to the same extent at steady state. Furthermore, we found that the half-lives of each of the proteins are also similar in these cells (~4−5 h), indicating that the glycosylation-deficient ABCG2 protein is not degraded more rapidly than its glycosylated counterpart.

The Glycosylation-Deficient Mutant ABCG2 (N596Q) Is an Active Drug-Stimulated ATPase. The basal and drug-stimulated ATPase activities of ABCG2 and the glycosylation-deficient ABCG2 (N596Q) variant were measured in crude membrane preparations prepared from transiently transfected/infected HeLa cells (Figure 6). The drug prazosin (20 μM), a substrate for ABCG2 (R482G) (*30*), was used to stimulate the ATPase activity. The negative control membranes, containing the empty vector pTM1, show a basal activity of approximately 6.5 ± 1.6 nmol π min^{-1} mg^{-1} and

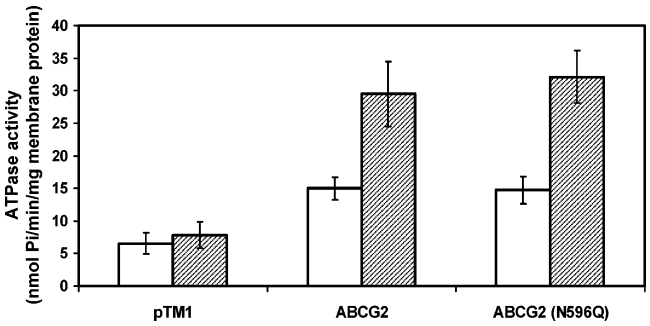

FIGURE 6: Drug-stimulated ATPase activity of ABCG2 and the glycosylation-deficient variant ABCG2 (N596Q). Vanadate-sensitive ATPase hydrolysis was measured as free phosphate release in crude membrane extracts (10 μg) from transiently transfected HeLa cells expressing either pTM1, ABCG2, or ABCG2 (N596Q) as described in Experimental Procedures. The assays were performed in both the absence (open bars) and presence (hatched bars) of 20 μM prazosin, resulting in basal and drug-stimulated activities, respectively. The activities from three independent experiments done in quadruplicate are shown (mean ± SD).

exhibit no prazosin-stimulated ATPase activity (7.9 ± 2.0 nmol π min^{-1} mg^{-1}) (Figure 6). The glycosylated ABCG2 membranes have a basal activity of 15.0 ± 1.8 nmol min^{-1} mg^{-1} and a prazosin-stimulated activity of 29.5 ± 5.0 nmol min^{-1} mg^{-1}, an approximate 2-fold stimulation (Figure 6). The glycosylation-deficient ABCG2 (N596Q) membranes have a basal activity of approximately 14.8 ± 2.1 nmol min^{-1} mg^{-1} and a prazosin-stimulated activity of 32.1 ± 4.0 nmol min^{-1} mg^{-1}, also an approximate 2-fold stimulation (Figure 6). Immunoblot analysis demonstrated that equal amounts of protein were expressed in the membrane preparations used for these experiments (data not shown). For this expression comparison, both samples were treated with PNGase F to eliminate the protein heterogeneity seen in the glycosylated sample and allow for a more accurate determination of expression.

The Glycosylation-Deficient ABCG2 (N596Q) Protein Is Expressed at the Cell Surface and Is Functional for Rhodamine 123 Transport. To determine if the glycosylation-deficient ABCG2 (N596Q) has cell surface expression and transport properties that are different from the glycosylated protein, we performed cell surface analysis and a time course analysis of rhodamine 123 transport. Cell surface expression experiments demonstrated that the glycosylation-deficient mutant is expressed similarly at the cell surface compared to the glycosylated ABCG2 protein (Figure 7A). Since these flow cytometry data describe the fluorescence of an entire population of cells, we also used confocal microscopy analysis in fixed, but not permeabilized, cells to detect only the cell surface expressed ABCG2 (Figure 7B). Using the extracellular epitope-specific monoclonal antibody 5D3 and a FITC-conjugated anti-mouse secondary antibody, individual cells overexpressing glycosylated ABCG2 showed surface punctuate fluorescence similar to cells overexpressing the glycosylation-deficient ABCG2 (N596Q) protein; compare glycosylated ABCG2 expressing cells in the top panel of Figure 7B (right) to the cell expressing ABCG2 (N596Q) in the bottom left of the lower panel of Figure 7B (right). These data corroborate the flow cytometry data and suggest that lack of glycosylation itself does not significantly affect trafficking of ABCG2 to the plasma membrane.

To assess function, a time course analysis of rhodamine 123 accumulation was performed on a portion of the same cell samples (Figure 8). The ABCG2 (N596Q) mutant is capable of transporting rhodamine 123 to the same extent as the glycosylated protein after 40 min (Figures 8C,D). However, slight differences in the amount of rhodamine 123 transported by the two transporters are observed at 10 and 20 min time points (Figures 8A,B), perhaps indicative of a subtle transport defect inherent to the nonglycosylated protein. These data strongly suggest that glycosylation is not essential for the overall transport function of ABCG2 but may have subtle detrimental effects. Since functional ABCG2 is thought to be a dimer or higher order oligomer (*10*−*12*), these data also suggest that glycosylation is not essential for the assembly of ABCG2.

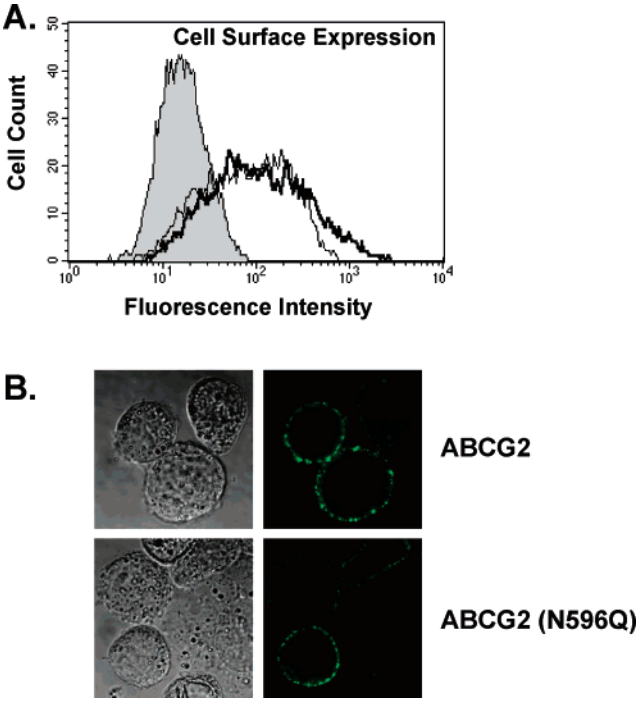

FIGURE 7: Cell surface expression of ABCG2 in HeLa cells expressing ABCG2 or the glycosylation-deficient variant ABCG2 (N596Q). HeLa cells were cotransfected/infected with the empty vector pTM1 (shaded peak), ABCG2 (—), or ABCG2 (N596Q) (—) and incubated for 21 h at 32 °C. (A) Cell surface expression of ABCG2 was assessed by flow cytometry as described in Experimental Procedures using the ABCG2-specific monoclonal antibody 5D3. (B) Cell surface expression of ABCG2 was assessed by confocal immunofluorescence microscopy in fixed, but not permeabilized, cells as described in Experimental Procedures. The images on the left side of the figure represent the nonfluorescent confocal transmission images of the cells. The images on the right side of the figure represent the same cells stained with the ABCG2-specific monoclonal antibody 5D3 and visualized with a FITC-conjugated anti-mouse secondary antibody.

DISCUSSION

Our studies demonstrate that ABCG2 transiently expressed in HeLa cells and ABCG2 (R482T) overexpressed in the drug-selected cell line, MCF-7/AdVp3000, are N-linked glycosylated. Upon removal of glycosylation with PNGase F or inhibition of N-linked glycosylation upon protein expression in the presence of tunicamycin, glycosylation-deficient ABCG2 migrates as a single band at a lower apparent molecular mass of approximately 60 kDa. Although there are three potential glycosylation sites in human ABCG2 at positions 418, 557, and 596, we have shown using site-directed mutagenesis that only the N596 site is glycosylated. Our flow cytometric analyses showed cell surface expression for ABCG2-transfected cells treated with tunicamycin and for the glycosylation-deficient mutant ABCG2 (N596Q) that was nearly equivalent to the fully glycosylated ABCG2 protein. Confocal microscopy images of transiently transfected HeLa cells with ABCG2 or ABCG2 (N596Q) demonstrated the same results qualitatively (data not shown), with individual cells expressing the glycosylation-deficient ABCG2 (N596Q) showing a similar punctuate fluorescence pattern at the plasma membrane to cells expressing glycosylated ABCG2.

The presence of a glycosylation site at asparagine 596 in the third extracellular loop of ABCG2 is the first direct evidence that supports the current topological model (*9*) (Swiss-Prot Q9UNQ0). According to the predicted model, N418 and N557 are located one to three residues from the

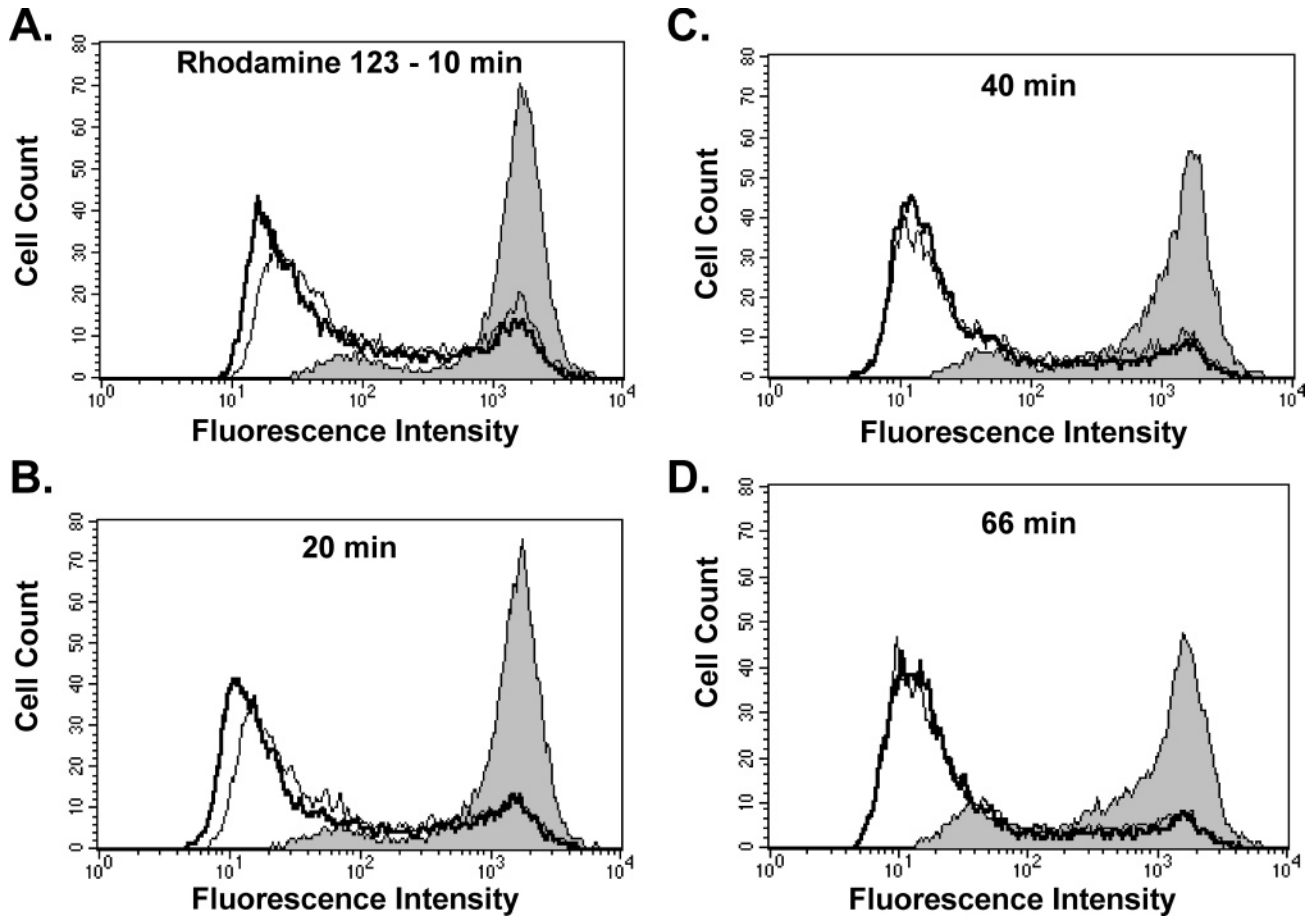

FIGURE 8: Time-dependent rhodamine 123 transport in HeLa cells expressing ABCG2 or the glycosylation-deficient variant ABCG2 (N596Q). HeLa cells were cotransfected/infected with the empty vector pTM1 (shaded peak), ABCG2 (—), or ABCG2 (N596Q) (−) and incubated for 21 h at 32 °C. Cellular rhodamine 123 accumulation was assessed as described in Experimental Procedures. Cells were first incubated at 37 °C for 40 min in the presence of 0.5 μg/mL rhodamine 123. Cells were subsequently incubated in drug-free medium at 37 °C for the times indicated: A = 10 min; B = 20 min; C = 40 min; D = 66 min. Following the incubation, cells were collected by centrifugation, and flow cytometry was performed as described in Experimental Procedures. Each histogram is based on a sample of 10000 cells, and each experiment was performed a minimum of three independent times.

transmembrane domains. For N-linked glycosylation of membrane-associated proteins, the minimal distance from the lumenal end of a transmembrane segment has been determined to be between twelve and fifteen residues, depending on whether the site is upstream or downstream of the transmembrane segment (*31*). Therefore, it is not surprising that the potentially glycosylated amino acids positioned near the membrane are not modified. In addition, sequence comparisons demonstrate that the ABCG2 sequences from mouse and rat do not have potential sites at positions 418 and 557 but do have an additional potential site at N600 that is not present in the human sequence. Importantly, only the glycosylation site identified in this study at asparagine 596 is conserved across multiple species. Using the LALIGN algorithm, amino acid sequence alignment comparisons between the entire third extracellular loop of human ABCG2 and mouse and rat ABCG2 proteins indicated 76.6% sequence identity over the 77 amino acids and 90.9% identity between the mouse and rat proteins (*32*). This high degree of conservation of the amino acids in this loop suggests an important function for this region. In addition to forming an accessible glycosylation site, this loop may also define an interface for homooligomerization or be involved in interactions with other proteins or cells.

In previous studies, it has been shown that the lack of glycosylation affected neither the drug transport function of ABC multidrug transporters, P-gp and MRP1, nor the substrate specificity of those transporters (*33*−*36*). Human ABCG2 has been expressed successfully in both insect cells and *Lactococcus lactis* in biologically active forms despite their lack of glycosylation (*24*, *30*, *37*). In this study, we show that the lack of glycosylation does not result in a significant decrease in total and cell surface expression of ABCG2. Furthermore, we found that the lack of glycosylation did not inhibit the ability of the protein to demonstrate both drug-stimulated ATPase activity and rhodamine 123 efflux in mammalian cells. Even though glycosylation-deficient P-gp was found to be expressed less well at the cell surface in mammalian cells (*36*), cells expressing this form of P-gp had drug resistance patterns that were indistinguishable from that of wild-type P-gp (*25*). Previous [^{35}S]-methionine/cysteine pulse−chase labeling studies also done with P-gp have shown that although the half-life was not affected, the glycosylation-deficient mutant incorporated less of the ^{35}S label due to degradation of misfolded mutant proteins by both the proteasome and endoplasmic reticulum-associated proteases (*36*). In contrast, we have shown in this study that the steady-state expression and half-life of the

glycosylation-deficient mutant ABCG2 (N596Q) protein are comparable to its glycosylation-competent counterpart.

Numerous studies suggest that glycosylation may play a role in targeting several ABC transporters to the cell surface by allowing proper folding of the polypeptide chain (*25*, *36*). The lack of N-linked oligosaccharides could slow the exit of the protein from the ER due to prolonged or increased interactions with ER chaperones such as the lectin calnexin or other processing enzymes (*38*). These enhanced interactions might hinder proper folding, which is essential for protein processing and routing to the plasma membrane. It is known that P-gp interacts with calnexin and that longer interactions with calnexin are observed for the P-gp glycosylation-deficient mutant (*38*). Also both of the half-transporters ABCG5 and ABCG8 are bound by calnexin, which may facilitate folding of obligate ABCG5/ABCG8 heterodimers (*39*). Additionally, it has been shown that N-linked glycosylation of the half-transporter ABCG8 was not required for dimerization with ABCG5 but was required for efficient trafficking of the ABCG5/ABCG8 heterodimer (*39*−*41*). Interestingly, although both ABCG5 and ABCG8 are glycosylated, only the glycosylation of ABCG8 was necessary for efficient trafficking of the complex to the cell membrane (*39*). In this study, we show that glycosylation is not essential for trafficking and function of ABCG2. We also demonstrated via Endo H digestion studies that the majority of expressed glycosylated ABCG2 was modified by complex glycosylation, suggesting that much of the expressed protein has exited the ER/*cis*-Golgi. Therefore, although ABCG2 is also presumed to be a dimer or higher order oligomer (*10*, *11*, *42*), glycosylation does not appear to be essential for assembly or trafficking the higher order complex to the cell surface. Furthermore, recent data from our laboratory show ABCG2 (N596Q) protein as a mixture of monomers and higher order oligomers, mostly dimers, on nonreducing SDS−PAGE gels (A. Bhatia and C. A. Hrycyna, unpublished data). Taken together, these results suggest that some but not all ABC transporters require glycosylation, suggesting that the role of this modification is not universal and must be examined for each transporter individually.

Several human diseases are caused by mutations that prevent the proper folding and exiting of ABC transporters out of the endoplasmic reticulum (*43*, *44*). A prominent example of this phenomenon is cystic fibrosis, where 90% of individuals affected by the disease express at least one copy of the gene encoding a deletion at phenylalanine 508 (ΔF508) that prevents the cystic fibrosis transmembrane regulator (CFTR) transporter from reaching the plasma membrane (*45*−*51*). Another example is sitosterolemia, an autosomal recessive disorder caused by mutations in ABCG5 and ABCG8 and characterized by sterol accumulation and premature atherosclerosis (*52*, *53*). ABCG5 and ABCG8 are half ABC transporters that must heterodimerize to move to the apical surfaces of enterocytes and hepatocytes (*40*, *41*). Recently, it was found that the majority of disease-causing mutations in ABCG5 and ABCG8 impair transport of the ABCG5/ABCG8 heterodimer to the cell surface (*39*). Novel strategies to promote proper folding and localization of ABC transporters may prove to be beneficial for the treatment of these and other diseases. For example, trafficking-deficient P-gp variants have been rescued by the addition of drug substrates or modulators such as capsaicin, cyclosporin A, vinblastine, or verapamil, resulting in the appearance of a fully glycosylated and functional protein at the cell surface (*54*).

The presence of glycosylation is generally considered to be contraindicated for successful three-dimensional structural analyses of proteins, and this effect is amplified for membrane proteins. In fact, once purified, the oligosaccharides are often enzymatically removed from the proteins before attempting crystallization. The results presented here demonstrate that glycosylation is not essential for the transport function and gross conformation of human ABCG2. These data, taken together with the fact that the glycosylation-deficient protein population appears to be homogeneous, suggests that it should be possible to generate large quantities of ABCG2 for three-dimensional crystallographic analyses in both mammalian and microbial systems.

REFERENCES

1. Dean, M., and Allikmets, R. (1995) Evolution of ATP-binding cassette transporter genes, *Curr. Opin. Genet. Dev. 5*, 779−785.
2. Allikmets, R., Gerrard, B., Hutchinson, A., and Dean, M. (1996) Characterization of the human ABC superfamily: isolation and mapping of 21 new genes using the expressed sequence tags database, *Hum. Mol. Genet. 5*, 1649−1655.
3. Higgins, C. F. (1992) ABC transporters: from microorganisms to man, *Annu. Rev. Cell. Biol. 8*, 67−113.
4. Gottesman, M. M., and Pastan, I. (1993) Biochemistry of multidrug resistance mediated by the multidrug transporter, *Annu. Rev. Biochem. 62*, 385−427.
5. Borst, P., Evers, R., Kool, M., and Wijnholds, J. (2000) A family of drug transporters: the multidrug resistance-associated proteins, *J. Natl. Cancer Inst. 92*, 1295−1302.
6. Miyake, K., Mickley, L., Litman, T., Zhan, Z., Robey, R., Cristensen, B., Brangi, M., Greenberger, L., Dean, M., Fojo, T., and Bates, S. E. (1999) Molecular cloning of cDNAs which are highly overexpressed in mitoxantrone-resistant cells: demonstration of homology to ABC transport genes, *Cancer Res. 59*, 8−13.
7. Doyle, L. A., Yang, W., Abruzzo, L. V., Krogmann, T., Gao, Y., Rishi, A. K., and Ross, D. D. (1998) A multidrug resistance transporter from human MCF-7 breast cancer cells, *Proc. Natl. Acad. Sci. U.S.A. 95*, 15665−15670.
8. Allikmets, R., Schriml, L. M., Hutchinson, A., Romano-Spica, V., and Dean, M. (1998) A human placenta-specific ATP-binding cassette gene (ABCP) on chromosome 4q22 that is involved in multidrug resistance, *Cancer Res. 58*, 5337−5339.
9. Ejendal, K. F., and Hrycyna, C. A. (2002) Multidrug resistance and cancer: the role of the human ABC transporter ABCG2, *Curr. Protein Pept. Sci. 3*, 503−511.
10. Kage, K., Tsukahara, S., Sugiyama, T., Asada, S., Ishikawa, E., Tsuruo, T., and Sugimoto, Y. (2002) Dominant-negative inhibition of breast cancer resistance protein as drug efflux pump through the inhibition of S−S dependent homodimerization, *Int. J. Cancer 97*, 626−630.
11. Litman, T., Jensen, U., Hansen, A., Covitz, K. M., Zhan, Z., Fetsch, P., Abati, A., Hansen, P. R., Horn, T., Skovsgaard, T., and Bates, S. E. (2002) Use of peptide antibodies to probe for the mitoxantrone resistance-associated protein MXR/BCRP/ABCP/ABCG2, *Biochim. Biophys. Acta 1565*, 6−16.
12. Xu, J., Liu, Y., Yang, Y., Bates, S., and Zhang, J. T. (2004) Characterization of oligomeric human half-ABC transporter ATP-binding cassette G2, *J. Biol. Chem. 279*, 19781−19789.
13. Cisternino, S., Mercier, C., Bourasset, F., Roux, F., and Scherrmann, J. M. (2004) Expression, up-regulation, and transport activity of the multidrug-resistance protein Abcg2 at the mouse blood-brain barrier, *Cancer Res. 64*, 3296−3301.
14. Allikmets, R., and Dean, M. (1998) Cloning of novel ABC transporter genes, *Methods Enzymol. 292*, 116−130.
15. Maliepaard, M., Scheffer, G. L., Faneyte, I. F., van Gastelen, M. A., Pijnenborg, A. C., Schinkel, A. H., van De Vijver, M. J., Scheper, R. J., and Schellens, J. H. (2001) Subcellular localization and distribution of the breast cancer resistance protein transporter in normal human tissues, *Cancer Res. 61*, 3458−3464.

16. Jonker, J. W., Smit, J. W., Brinkhuis, R. F., Maliepaard, M., Beijnen, J. H., Schellens, J. H., and Schinkel, A. H. (2000) Role of breast cancer resistance protein in the bioavailability and fetal penetration of topotecan, *J. Natl. Cancer Inst. 92*, 1651−1656.
17. Taipalensuu, J., Tornblom, H., Lindberg, G., Einarsson, C., Sjoqvist, F., Melhus, H., Garberg, P., Sjostrom, B., Lundgren, B., and Artursson, P. (2001) Correlation of gene expression of 10 drug efflux proteins of the ATP-binding cassette transporter family in normal human jejunum and in human intestinal epithelial Caco-2 cell monolayers, *J. Pharmacol. Exp. Ther. 299*, 164−170.
18. Zhou, S., Schuetz, J. D., Bunting, K. D., Colapietro, A. M., Sampath, J., Morris, J. J., Lagutina, I., Grosveld, G. C., Osawa, M., Nakauchi, H., and Sorrentino, B. P. (2001) The ABC transporter Bcrp1/ABCG2 is expressed in a wide variety of stem cells and is a molecular determinant of the side-population phenotype, *Nat. Med. 7*, 1028−1034.
19. Scharenberg, C. W., Harkey, M. A., and Torok-Storb, B. (2002) The ABCG2 transporter is an efficient Hoechst 33342 efflux pump and is preferentially expressed by immature human hematopoietic progenitors, *Blood 99*, 507−512.
20. Jonker, J. W., Buitelaar, M., Wagenaar, E., Van Der Valk, M. A., Scheffer, G. L., Scheper, R. J., Plosch, T., Kuipers, F., Elferink, R. P., Rosing, H., Beijnen, J. H., and Schinkel, A. H. (2002) The breast cancer resistance protein protects against a major chlorophyll-derived dietary phototoxin and protoporphyria, *Proc. Natl. Acad. Sci. U.S.A. 99*, 15649−15654.
21. Doyle, L. A., and Ross, D. D. (2003) Multidrug resistance mediated by the breast cancer resistance protein BCRP (ABCG2), *Oncogene 22*, 7340−7358.
22. Imai, Y., Tsukahara, S., Ishikawa, E., Tsuruo, T., and Sugimoto, Y. (2002) Estrone and 17beta-estradiol reverse breast cancer resistance protein-mediated multidrug resistance, *Jpn. J. Cancer Res. 93*, 231−235.
23. Imai, Y., Asada, S., Tsukahara, S., Ishikawa, E., Tsuruo, T., and Sugimoto, Y. (2003) Breast cancer resistance protein exports sulfated estrogens but not free estrogens, *Mol. Pharmacol. 64*, 610−618.
24. Janvilisri, T., Venter, H., Shahi, S., Reuter, G., Balakrishnan, L., and van Veen, H. W. (2003) Sterol transport by the human breast cancer resistance protein (ABCG2) expressed in *Lactococcus lactis*, *J. Biol. Chem. 278*, 20645−20651.
25. Schinkel, A. H., Kemp, S., Dolle, M., Rudenko, G., and Wagenaar, E. (1993) N-glycosylation and deletion mutants of the human MDR1 P-glycoprotein, *J. Biol. Chem. 268*, 7474−7481.
26. Hrycyna, C. A., Ramachandra, M., Pastan, I., and Gottesman, M. M. (1998) Functional expression of human P-glycoprotein from plasmids using vaccinia virus-bacteriophage T7 RNA polymerase system, *Methods Enzymol. 292*, 456−473.
27. Zhou, S., Zong, Y., Lu, T., and Sorrentino, B. P. (2003) Hematopoietic cells from mice that are deficient in both Bcrp1/Abcg2 and Mdr1a/1b develop normally but are sensitized to mitoxantrone, *BioTechniques 35*, 1248−1252.
28. Honjo, Y., Hrycyna, C. A., Yan, Q. W., Medina-Perez, W. Y., Robey, R. W., van De Laar, A., Litman, T., Dean, M., and Bates, S. E. (2001) Acquired mutations in the mxr/bcrp/abcp gene alter substrate specificity in mxr/bcrp/abcp-overexpressing cells, *Cancer Res. 61*, 6635−6639.
29. Ramachandra, M., Ambudkar, S. V., Gottesman, M. M., Pastan, I., and Hrycyna, C. A. (1996) Functional characterization of a glycine 185-to-valine substitution in human P-glycoprotein by using a vaccinia-based transient expression system, *Mol. Biol. Cell 7*, 1485−1498.
30. Özvegy, C., Litman, T., Szakacs, G., Nagy, Z., Bates, S., Varadi, A., and Sarkadi, B. (2001) Functional characterization of the human multidrug transporter, ABCG2, expressed in insect cells, *Biochem. Biophys. Res. Commun. 285*, 111−117.
31. Nilsson, I. M., and von Heijne, G. (1993) Determination of the distance between the oligosaccharyltransferase active site and the endoplasmic reticulum membrane, *J. Biol. Chem. 268*, 5798−5801.
32. Huang, X., and Miller, W. (1991) LALIGN Alignment Server, *Adv. Appl. Math. 12*, 373−381.
33. Schinkel, A. H., Arceci, R. J., Smit, J. J. M., Wagenaar, E., Baas, F., Dolle, M., Tsuruo, T., Mechetner, E. B., Roninson, I. B., and Borst, P. (1993) Binding properties of monoclonal antibodies recognizing external epitopes of the human MDR1 P-glycoprotein, *Int. J. Cancer 55*, 478−484.
34. Hipfner, D. R., Almquist, K. C., Leslie, E. M., Gerlach, J. H., Grant, C. E., Deeley, R. G., and Cole, S. P. (1997) Membrane topology of the multidrug resistance protein (MRP). A study of glycosylation-site mutants reveals an extracytosolic NH2 terminus, *J. Biol. Chem. 272*, 23623−23630.
35. Bakos, E., Hegedus, T., Hollo, Z., Welker, E., Tusnady, G. E., Zaman, G. J., Flens, M. J., Varadi, A., and Sarkadi, B. (1996) Membrane topology and glycosylation of the human multidrug resistance-associated protein, *J. Biol. Chem. 271*, 12322−12326.
36. Gribar, J. J., Ramachandra, M., Hrycyna, C. A., Dey, S., and Ambudkar, S. V. (2000) Functional characterization of glycosylation-deficient human P-glycoprotein using a vaccinia virus expression system, *J. Membr. Biol. 173*, 203−214.
37. Özvegy, C., Varadi, A., and Sarkadi, B. (2002) Characterization of drug transport, ATP hydrolysis, and nucleotide trapping by the human ABCG2 multidrug transporter. Modulation of substrate specificity by a point mutation, *J. Biol. Chem. 277*, 47980−47990.
38. Loo, T. W., and Clarke, D. M. (1994) Prolonged association of temperature-sensitive mutants of human P-glycoprotein with calnexin during biogenesis, *J. Biol. Chem. 269*, 28683−28689.
39. Graf, G. A., Cohen, J. C., and Hobbs, H. H. (2004) Missense mutations in ABCG5 and ABCG8 disrupt heterodimerization and trafficking, *J. Biol. Chem. 279*, 24881−24888.
40. Graf, G. A., Li, W. P., Gerard, R. D., Gelissen, I., White, A., Cohen, J. C., and Hobbs, H. H. (2002) Coexpression of ATP-binding cassette proteins ABCG5 and ABCG8 permits their transport to the apical surface, *J. Clin. Invest. 110*, 659−669.
41. Graf, G. A., Yu, L., Li, W. P., Gerard, R., Tuma, P. L., Cohen, J. C., and Hobbs, H. H. (2003) ABCG5 and ABCG8 are obligate heterodimers for protein trafficking and biliary cholesterol excretion, *J. Biol. Chem. 278*, 48275−48282.
42. Xu, J., Liu, Y., Yang, Y., Bates, S., and Zhang, J. T. (2004) Characterization of oligomeric human half ABC transporter ABCG2/BCRP/MXR/ABCP in plasma membranes, *J. Biol. Chem. 279*, 19781−19789.
43. Aridor, M., and Hannan, L. A. (2000) Traffic jam: a compendium of human diseases that affect intracellular transport processes, *Traffic 1*, 836−851.
44. Aridor, M., and Hannan, L. A. (2002) Traffic jams II: an update of diseases of intracellular transport, *Traffic 3*, 781−790.
45. Ko, Y. H., and Pedersen, P. L. (2001) Cystic fibrosis: a brief look at some highlights of a decade of research focused on elucidating and correcting the molecular basis of the disease, *J. Bioenerg. Biomembr. 33*, 513−521.
46. Welsh, M. J., Denning, G. M., Ostedgaard, L. S., and Anderson, M. P. (1993) Dysfunction of CFTR bearing the delta F508 mutation, *J. Cell. Sci., Suppl. 17*, 235−239.
47. Fuller, C. M., and Benos, D. J. (1992) Cftr!, *Am. J. Physiol. 263*, C267−C286.
48. Brown, P. C., Thorgeirsson, S. S., and Silverman, J. A. (1993) Cloning and regulation of the rat mdr2 gene, *Nucleic Acids Res. 21*, 3885−3891.
49. Kopito, R. R. (1999) Biosynthesis and degradation of CFTR, *Physiol. Rev. 79*, S167−S173.
50. Cheng, S. H., Gregory, R. J., Marshall, J., Paul, S., Souza, D. W., White, G. A., O'Riordan, C. R., and Smith, A. E. (1990) Defective intracellular transport and processing of CFTR is the molecular basis of most cystic fibrosis, *Cell 63*, 827−834.
51. Gelman, M. S., and Kopito, R. R. (2002) Rescuing protein conformation: prospects for pharmacological therapy in cystic fibrosis, *J. Clin. Invest. 110*, 1591−1597.
52. Shulenin, S., Schriml, L. M., Remaley, A. T., Fojo, S., Brewer, B., Allikmets, R., and Dean, M. (2001) An ATP-binding cassette gene (ABCG5) from the ABCG (White) gene subfamily maps to human chromosome 2p21 in the region of the Sitosterolemia locus, *Cytogenet. Cell Genet. 92*, 204−208.
53. Berge, K. E., Tian, H., Graf, G. A., Yu, L., Grishin, N. V., Schultz, J., Kwiterovich, P., Shan, B., Barnes, R., and Hobbs, H. H. (2000) Accumulation of dietary cholesterol in sitosterolemia caused by mutations in adjacent ABC transporters, *Science 290*, 1771−1775.
54. Loo, T. W., and Clarke, D. M. (1997) Correction of defective protein kinesis of human P-glycoprotein mutants by substrates and modulators, *J. Biol. Chem. 272*, 709−712.
55. Laemmli, U. K. (1970) Cleavage of structural proteins during the assembly of the head of bacteriophage T4, *Nature 227*, 680−685.

BI0479858